

EXPLORING THERMAL RESPONSE IN ALUMINUM HEAT SINKS WITH VARIABLE SURFACE ROUGHNESS FOR ENHANCED COOLING

by

**Rajasekaran BALAKRISHNAN^{a*}, Kumaresan GOVINDARAJ^a,
Arulprakasajothi MAHALINGAM^b, and Beemkumar NAGAPPAN^c**

^aDepartment of Mechanical Engineering, Anna University Chennai, Tamil Nadu, India

^bDepartment of Mechanical Engineering, KCG College of Technology,
Chennai, Tamil Nadu, India

^cDepartment of Mechanical Engineering, Jain (Deemed-to-be) University,
Bangalore, Karnataka, India

Original scientific paper

<https://doi.org/10.2298/TSCI230916013B>

The shrinking size and increasing power consumption of electronic products also make their thermal management challenging. Poor thermal management results in increased temperature of the electronic component, ultimately leading to the failure of the element. Thermal management of electronic devices is assisted by-passive techniques such as heat sinks. Phase change material-filled heat sinks attract industries, as they are compact and do not require frequent maintenance. In this study, heat sinks with internal surface modifications, i.e., engraving and grit blasting, are developed. The heat sinks are provided with heat storage mediums like paraffin wax and nanoparticles to analyse their effect on thermal management. This study employed two different nanoparticles, i.e., silver titanium dioxide and graphene. A simple heat sink without surface modification and a heat storage medium was used as a reference. It was found that using graphene-mixed PCM in the smooth heat sink increased the charging time by about 8%. Adding graphene nanoparticles to the phase change material decreases the discharging time by about 29%. Grit-blasted heat sinks took the most time to discharge, followed by base-engraved heat sinks. This is because the internal surface roughened heat sinks stored more heat energy during the charging process. Adding graphene nanoparticles to the PCM increases the duty cycle by about 40%. When used with paraffin wax, base engraved heatsinks and grit-blasted heat sinks have increased the duty cycle by 11% and 36%, respectively.

Key words: *heat sinks, thermal management, surface modification, phase change material, nanoparticles*

Introduction

Rapid innovation in technology around the globe has resulted in the transformation of commercial goods. Many goods, such as computers, mobile phones, vehicles, toys, drones, and home appliances, function with the help of electronics [1]. Day by day, the size of the electronic components is shrinking while exhibiting more incredible processing speed and functioning abilities. Hence, they have to be adequately cooled to ensure their proper functioning. Heat sinks aid in cooling features like electronic devices, refrigerators, and air conditioners [2].

* Corresponding author, e-mail: brajasekaran23@gmail.com

Many researchers have studied the possibilities of using PCM for heat transfer in electronic devices [3-5]. Typically, PCM relies on the latent heat transfer that occurs while the substance undergoes a phase change, *i.e.*, melting and solidification. Unlike sensible heat transfer, latent heat transfer exhibits enhanced energy transfer. This phenomenon is effectively used for condensers, evaporators, refrigeration and air conditioning applications [6].

Rajesh and Balaji [7] developed a study on phase changes due to the heating and cooling of the compound with constant power levels of 5-10 W corresponding to fluxes of 2-4 kW/m². They used a plate heat sink with fins and *n*-eicosane as a PCM. It has been shown that the performance can be compared when PCM are installed on the heat sinks and without. For up to 90 minutes of operation, the PCM could keep the surface temperature of the heat sink within 50 °C during the process.

The study by Pal and Joshi [8] looked at the behaviour of *n*-triacontane under constant heat loads both experimentally and numerically. The study correlated natural-convection with PCM and PCM with natural-convection, resulting in a correlation between the two variables. During the initial stages of melting, natural-convection was reported by the authors to be one of the dominant processes that govern melting. It was shown by Kandasamy *et al.* [9] that heat sinks with paraffin could perform transient cooling better than non-paraffin heat sinks. During their study of natural-convection, they found that, at lower power levels, the influence of PCM was not sensed. This is because of PCM sufficiently high melting point (55-60 °C). This temperature range is higher than the natural-convection temperature of the heat sink (24-28 °C).

There have been studies done by Fok *et al.* [10] with eicosane as a PCM to produce a similar analysis, and they found that as PCM, eicosane was influential in the lower power range (3-5 W) due to its lower melting point of 35-40 °C. According to Yang and Wang [11], a numerical study was conducted using *n*-eicosane as a PCM for power levels ranging from 2-4 W. The temperature of PCM can be maintained around 50-60 °C by using an aluminum heat sink, and the orientation of the PCM does not have a significant impact on the melting process.

A few research works highlighted the benefits of adding nanoparticles in the PCM [12-14]. Choi *et al.* [15] used multi-walled CNT, graphite and graphene as TCM and found the thermal conductivity of the nanoenhanced PCM for thermal energy storage applications. In this study, polyvinylpyrrolidone was used as a surfactant and stearic acid was used as a PCM. It has also been found that PVP with a 0.1 vol.% concentration exhibits the highest thermal conductivity of 21.5%, in addition graphene. Bahiraei *et al.* [16] synthesised graphene nanoplatelets, graphite nanoplatelets, and carbon nanofibers using paraffin wax as a PCM. Among the NePCM tested, those based on graphite, with mass fractions ranging between 7.5% and 10%, performed better in thermal management applications. Zou *et al.* [17] prepared and studied the thermal conductivity of multi-walled carbon nano tubes (MWCNT), graphene, and MWCNT/graphene-based NePCM using paraffin wax as the PCM and compared them to the thermal conductivity of paraffin wax. There was a significant increase in thermal conductivity in the hybrid NePCM based on MWCNT and graphene.

When PCM and paraffin RT50 were dispersed with 2 and 4 weight percent of CuO during phase transitions, Pahamli *et al.* [18] observed maximum changes in thermal conductivity of 3.9% and, respectively, during the phase transitions. Praveen and Suresh [19] have investigated a solid-solid neopentyl glycol and CuONePCM thermal management application using solid-solid neopentyl glycol and CuONePCM. When CuO was present at a weight percentage of 3.0 wt.% in the sample, achieving a maximum thermal conductivity of 0.61 W/mK was possible. Using this weight percentage, the phase change enthalpy was calculated to be 112.4 kJ/kg based on the weight percentage.

Sharma *et al.* [20] prepared NePCM that consisted of TiO₂ fractions of 0.5%, 1.0%, 3.0%, and 5% and palmitic acid that consisted of particles of 0.5%, 1.0%, 3.0%, and 5%. The thermal conductivity of TiO₂ with a weight percentage of 5.0 wt.% measured in this study was 0.35 W/mK, and the latent heat value calculated in this study was 180.03 kJ/kg, indicating maximum thermal conductivity. Putra *et al.* [21] prepared shape-stable PCM using bee wax as a PCM and MWCNT as a TCM, which were used to prepare shape-stable PCM. Using MWCNT with a weight ratio of five weight percent and twenty weight percent, the material's thermal conductivity was found to be 0.46 W/mK.

The NePCM was synthesised using myristic acids, and nanographite was dispersed with GNP, MWCNT, and nanographite at concentrations of 1 wt.%, 2 wt.%, and 3 wt.% as a PCM by He *et al.* [22]. There was a significant difference in the thermal performance of MWCNT and nanographite compared to the other two materials. There was an increase in thermal conductivity of 76.26%, 47.30%, and 44.0 %, respectively, when the concentration of GNP, MWCNT, and nanographite was increased to a weight concentration of 3 wt.%. Using *n*-eicosane as PCM, SiO₂ as supporting matrix, and EG as TCM, Zhang *et al.* [23] prepared NePCM at weight concentrations of 3 wt.%, 5 wt.%, and 7 wt.% by using *n*-eicosane as PCM and SiO₂ as supporting matrix. Considering the 7 wt.% amount of EG and the thermal conductivity enhancement, the melting, latent heat rate was 135.80 J/g, while the solidifying latent heat rate was 125.93 J/g.

Fin thickness plays a vital role in heat transfer through heat sinks. An experimental investigation evaluate electronic devices' cooling process revealed that 3 mm fin thickness reduced the base temperature by 28.3%. While using PCM, *i.e.*, PT 58, the thermal conductivity of the heat sink increased by 9%, respectively Lawang *et al.* [24]. Aerofoil-shaped fins enabled minimal flow resistance to the cooling fluid, facilitating enhanced heat transfer for active heat exchangers. It was revealed that the Nusselt number for heat sinks having a streamlined arrangement of fins was approximately 4% greater than its counterpart having a staggered arrangement of fins Babar *et al.* [25]. Varying concentrations of additives 3-6 wt.% like MWCNT were used in PCM, *i.e.*, RT-42. The square pin fins, the base temperature by 24% in the heat sink while using 6 wt.% of MWCNT in the PCM. However, the base temperature of its counterpart with circular pin fins was noted to be 26%, Fayyaz *et al.* [26]. This study examines the phenomenal influence of surface roughness and nanoparticles-infused PCM on the thermal energy management of heat sinks for electronic cooling.

Experimental work

Design of the heat sink

Figure 1 shows the geometry of the heat sink used for this study. The heat sink has a flat bottom surface, the four walls of the heat sink act as the extended surface to assist in heat transfer. The top of the heat sink is left open. This design facilitates the PCM control and allows heat transfer between the PCM and the atmosphere. Because of this design, the heat sink can be used only over stationary and horizontal surfaces.

Fabrication of the heat sink

The heat sinks used in this study are made of aluminum due to their beneficial properties like low

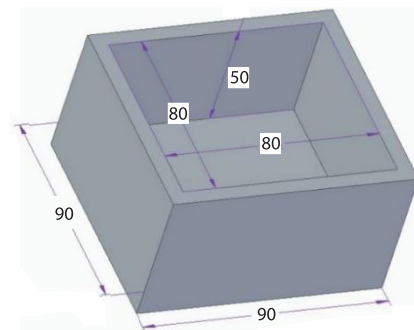


Figure 1. Dimensions [mm] of the heat sink

density, easy machinability, high thermal conductivity, thermal diffusivity and corrosion resistance. Five heat sinks were fabricated using CNC milling. One of the heat sinks, R1, is kept as a reference and is not subjected to any post-treatment process. Figure 2 shows the image of the fabricated heat sink. Surface modification, *i.e.*, roughening of the internal surfaces, was carried out on four heat sinks. Two heat sinks subjected to surface modification were engraved, while the others were grit blasted. Engraving was cost-effective compared to advanced manufacturing techniques like 3-D printing, laser cutting, wire cutting, and water jet cutting. Two different depths of cut are provided using a 0.5 mm diameter micro milling cutter as part of the engraving. The heat sink, R2, was engraved to give a 0.1 mm depth of cut. The heat sink, R3, was branded to provide a 0.2 mm depth of cut. Grit blasting was made using alumina, Al_2O_3 , grits that were pneumatically sprayed at 5 bar over the internal surfaces of the heat sink. The heat sink, R4, was subjected to grit blasting with the particles passing through a sieve (No. 46). The heat sink, R5, was subjected to grit blasting with the particles passing through a sieve (No. 16).

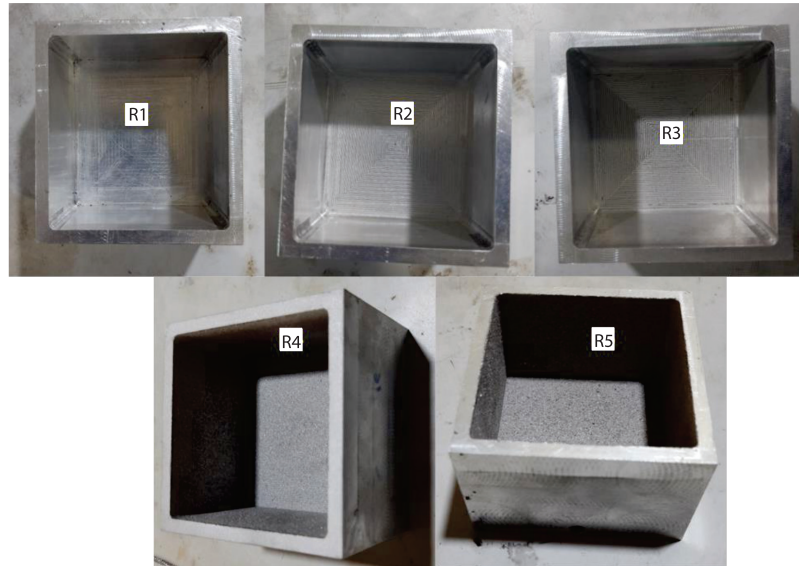


Figure 2. Fabricated heat sink

Measurement of surface roughness

The R_a is the arithmetic average roughness relative to the base length. This measures the average difference between peaks and valleys of the surface during the measurement period. The non-roughened heat sink is assumed to have smooth surfaces; hence, the R_a value of this heat sink is 0. The R_a values of the grit-blasted heat sinks were measured using a contact-type surface roughness tester, and the R_a values of base engraved heat sinks were measured using a non-contact-type surface roughness tester. The R_a values of all the five heat sinks were found:

$$R_a = \frac{1}{L} \int_0^L |Y| dx \quad (1)$$

where Y is the profile deviation from the centreline at any position x . The values obtained are presented in tab. 1.

Table 1. Roughness values of different heat sinks

Heat sink	R_a value
R1	0 μm
R2	6.6 μm
R3	33.9 μm
R4	10.4 μm
R5	15.2 μm

Synthesis of heat storage medium

Paraffin wax was chosen as the PCM for heat storage because of its low cost and non-toxicity. Graphene and AgTiO_2 nanoparticles were selected as thermal conductivity enhancers of paraffin wax, increasing the thermal conductivity of the paraffin wax when added. The high thermal conductivity of graphene and AgTiO_2 makes it the appropriate choice. The literature review showed that 4 wt.% by weight is the optimal quantity for which nanoparticles may be added to the PCM. Three different PCM were used for experimentation – Plain paraffin wax, Paraffin wax containing four wt.% graphene nanoparticles by weight and paraffin wax containing 4 wt.% AgTiO_2 nanoparticles by weight. Table 2 shows the properties of the base material and the PCM used for this study.

Table 2. Properties of aluminum and paraffin wax

Property	Aluminum	Paraffin wax (solid)	Paraffin wax (liquid)
Thermal conductivity [$\text{Wm}^{-1}\text{K}^{-1}$]	204.2	0.15	0.15
Density [kgm^{-3}]	2700	833.6	775
Specific heat [$\text{JKg}^{-1}\text{K}^{-1}$]	896	2384	2440
Thermal diffusivity [mm^2s^{-2}]	84.18	0.075	0.079
Kinematic viscosity [mm^2s^{-1}]	–	–	83.1
Prandtl number	–	–	1052
Volume expansivity [K^{-1}]	–	–	$7.14 \cdot 10^{-3}$

The PCM Paraffin Wax RT 58 – industrial grade, graphene nanoparticles and AgTiO_2 nanoparticles are commercially available and purchased from the market. To synthesise nano-enhanced PCM, a measured quantity of paraffin wax is melted in a heater, and 4% nanoparticles by weight are added to the melted PCM. To ensure uniform dispersion of nanoparticles in the PCM, the mixture is stirred for about 6 hours using a magnetic stirrer. The 200 g of the PCM is poured into the heat sink to solidify and cool to room temperature. Finally, we got a PCM/NePCM-filled heat sink, with which the experiments were performed. Figure 3 shows all three PCM filled in heat sinks, of which the central one is AgTiO_2 added PCM, the black-colored one is Graphene added PCM, and the white-colored one is plain paraffin wax.

Testing of heat sinks

A 35 W plate-type electric heater, which substitutes the heat supplied by the electronic component, is attached to the bottom of the PCM-filled heat sink. Wood is provided as insulating material below the heater to prevent heat loss from the bottom. A cubic housing of dimensions $0.3 \text{ m} \times 0.3 \text{ m} \times 0.3 \text{ m}$, made of acrylic sheets, is provided to simulate the actual scenario of

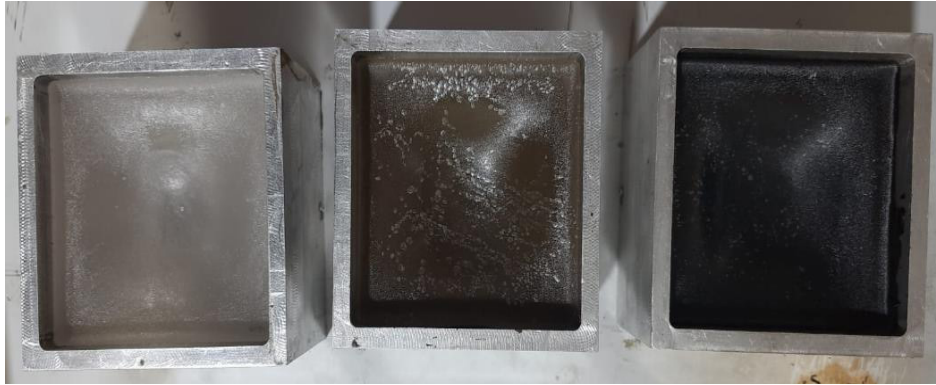


Figure 3. The PCM/Ne PCM-filled heat sinks

heat transfer, where the exposure of the heat sink to the ambient air is limited. This housing also acts as a convective enclosure, which prevents the fluctuation in surroundings from directly affecting our experiment's heat transfer. Four thermocouples are connected to measure the base plate temperature at four different points in the base plate.

A total of 15 experiments were conducted using a hybrid combination of three different PCM and five different heat sinks. The experiments include filling the heat sink with 200 g of the desired PCM, heating the heat sink with a 35 W plate heater, observing the time taken for the heat sink's temperature to rise to 70 °C, turning off the heater and observing the time taken by the heat sink to cool down to room temperature. All the experiments were performed in an isothermal room with a room temperature of 32 °C.

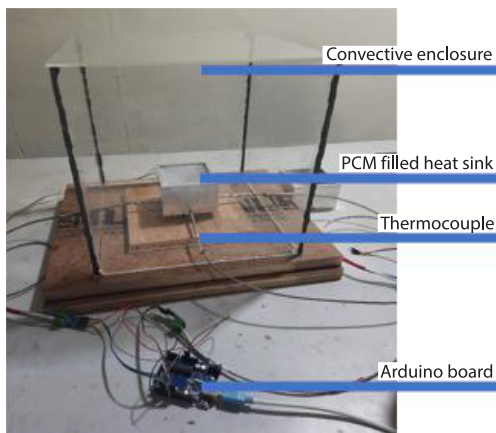


Figure 4. Experimental set-up used in the study

The average of these four temperature readings is the base plate temperature reading. The output from the Arduino board is directly fed into Microsoft Excel software, where it is recorded. The experiments were conducted in an isothermal room at 32 °C. The limiting temperature of the heat sink was kept at 70 °C. Hence, the time required for the heat sink to reach this temperature was recorded. After this temperature was reached, the heater was turned off, and then the temperature at which the heat sink reached room temperature was measured. To obtain the charging and discharging characteristics, the temperature is recorded every 30 seconds. The experimental set-up is shown in fig. 4.

Characterisation of PCM was done to describe the distinctive nature or features through different experiments. The SEM, differential scanning calorimetry (DSC), and thermo-gravimetric analysis (TGA) are the tests conducted on all three PCM samples to describe the nature of the synthesised PCM. Experiments were carried out in the reference heat sink, heat sinks subjected to surface roughness, and the heat sinks were provided with heat storage mediums. This study aims to determine each heat sink's specific charging and discharging cycle. To simplify the analysis, the temperature of the aluminum heat sink is assumed to be equal

at all points at any instant. Charging time is estimated using the equation of energy balance. Discharging time is calculated using plane front solidification equations and Biot analysis.

Results and discussion

Characterisation of the heat storage medium

The PCM samples were analysed using SEM to obtain information about the size and distribution of nanoparticles added to the PCM sample. The SEM images of the plain paraffin wax sample, graphene-added paraffin sample, and AgTiO₂-added paraffin sample are presented in fig. 5. The photos show that the dispersion of nanoparticles in the PCM samples is uniform, and the size of graphene nanoparticles and AgTiO₂ nanoparticles are of the order of 8 μm and 40 μm , respectively.

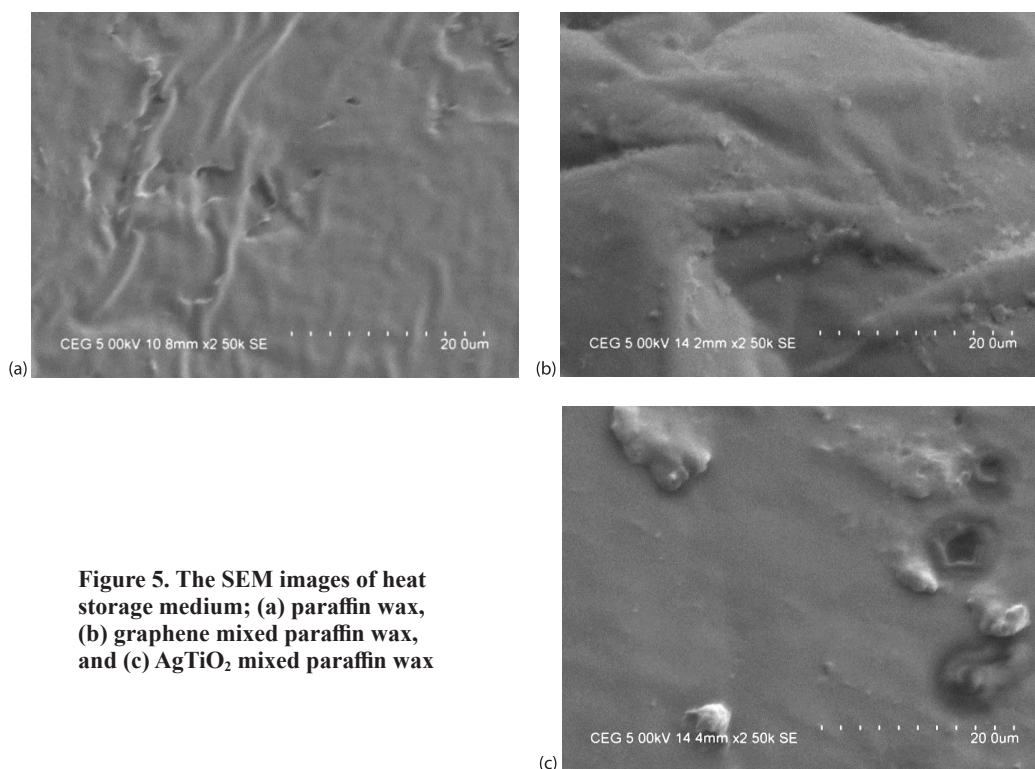


Figure 5. The SEM images of heat storage medium; (a) paraffin wax, (b) graphene mixed paraffin wax, and (c) AgTiO₂ mixed paraffin wax

The TGA is done to obtain a sample's weight vs. temperature plot when the sample is heated at a constant temperature ramp rate in a controlled environment. From this plot, the thermal decomposition temperature of the piece – the temperature at which the model starts to interact with the surroundings and lose weight, is determined. The TGA of all three samples was conducted at a temperature ramp rate of 20 K per minute from room temperature – 30-700 $^{\circ}\text{C}$, and the results are presented in fig. 6. From the plot, It can be inferred that all three samples are thermally stable up to 200 $^{\circ}\text{C}$, and beyond this temperature, all models start to decompose gradually. Hence, these paraffin waxes cannot be used for heat sink applications with a limiting temperature above 200 $^{\circ}\text{C}$.

The DSC is a thermo-analytical technique where the instantaneous rate of heat input required to raise the temperature of a sample at a constant ramp rate is measured over a range

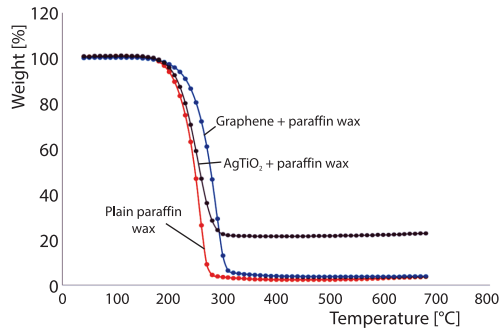


Figure 6. Thermo-gravimetric analysis

of temperatures. The DSC of PCM gives information about its melting content and latent heat of melting. The DSC of all three PCM samples was carried out in a liquid nitrogen environment, heating and cooling at a 2 K per minute ramp rate, over 30-90 °C. The inference of DSC of all three PCM samples is presented in tab. 3.

It can be seen from the previous table that there is no significant change in the melting range of PCM due to the addition of nanoparticles. However, the latent heat of melting decreases by about 20% due to the accumulation of nanoparticles.

Table 3. Melting range and latent heat of melting of the three PCM samples

PCM	Melting range	Latent heat of melting
Plain paraffin wax	56.1-66.3 °C	127.2 kJ/kg
Graphene added paraffin wax	59.3-64.8 °C	105.6 kJ/kg
AgTiO ₂ added paraffin wax	55.7-66.3 °C	101.1 kJ/kg

Analysis during heating of the heat sink

This study considers the heating cycle of the heat sink as a charging cycle. The effect of nanoenhancement of PCM, roughening of internal surfaces of the heat sink and a hybrid combination of both on the charging period of the heat sink, that is, the time taken for the heat sink to reach 70 °C, is discussed in this section. The time vs. temperature plot of five different heat sinks, comparing all three PCM is presented in fig. 7. These plots were drawn by recording the temperature of the heat sink every 30 seconds over the total cycle time, that is, both charging and discharging of the heat sink.

All these plots start from charging from time $t = 0$ second. The end of charging and beginning of discharging is marked by the point where the temperature is 70 °C, and the plot ends at the end of discharging. For every heat sink, the charging time is more when graphene-added paraffin wax is used. From the thermal management point of view, it is desirable to have a heat sink with a higher charging time. Therefore, we can conclude that graphene-added paraffin wax is the best-performing PCM in charging among all the three PCM used during charging. The reason for this is the higher thermal conductivity of graphene, which ultimately resulted in a higher convective heat transfer coefficient during heat transfer. The addition of nanoparticles reduces the latent heat of melting of the PCM, and enhanced thermal conductivity yielded better results than any other PCM during charging.

Different sets of plots were plotted using the same readings to understand the effect of roughening on the internal surfaces of the heat sink. In the new collection of stories, the time vs. temperature plots comparing all five heat sinks, when filled in the same PCM, were plotted. These plots are shown in fig. 8. From these plots, we can conclude that R5 is the best heat sink out of all five heat sinks in terms of charging. The R5 heat sink has the highest charging period among all other heat sinks and is independent of the choice of PCM. Grit-blasted heat sinks are also seen to perform best, followed by base-engraved heat sinks. It is also noticed that the higher the R_a value of the heat sink, the higher the charging time, and it is independent of the roughening method.

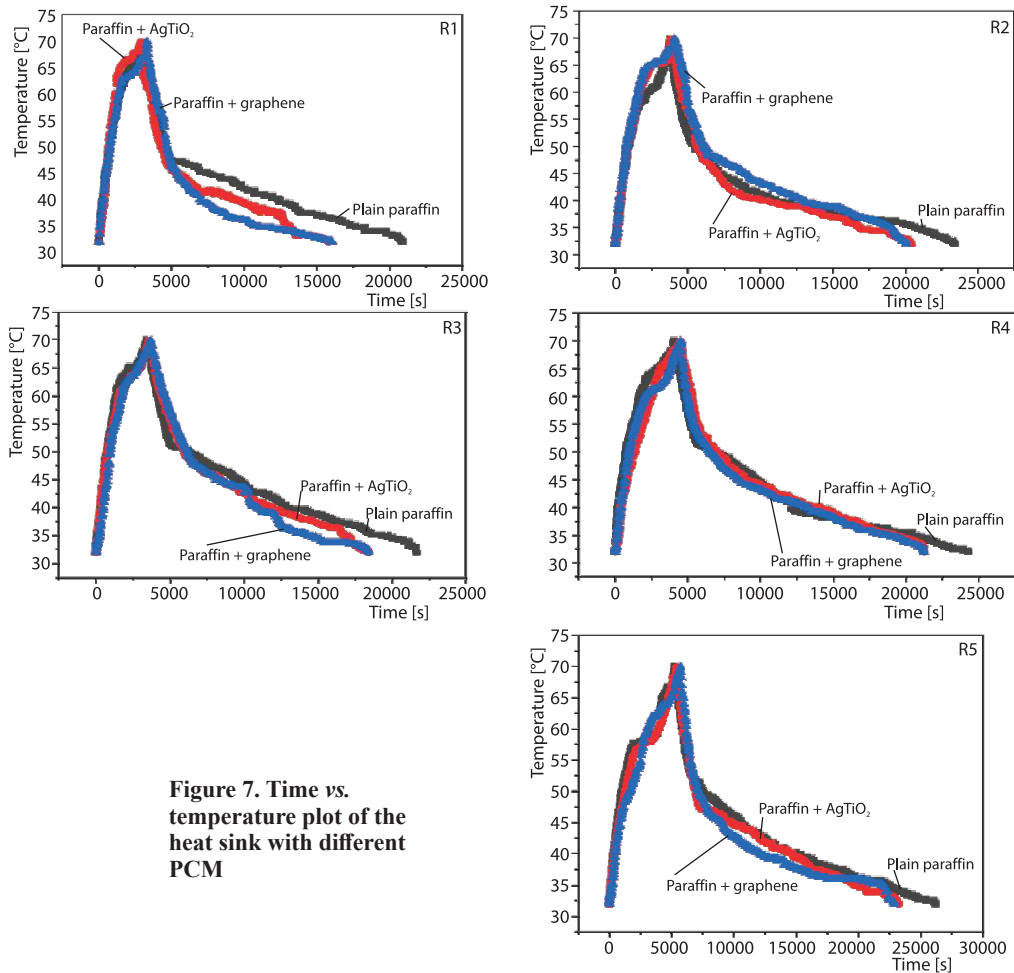


Figure 7. Time vs. temperature plot of the heat sink with different PCM

Graphene mixed PCM in the smooth heat sink, *i.e.*, R1, increases the charging time by about 8%. Using a grit-blasted heat sink instead of a smooth heat sink can increase the charging time by up to 70%, and using a base engraved heat sink can increase the charging time by about 25%. A hybrid combination of grit blasting and graphene nanoenhancement of the PCM gives the best charging performance. The increase in charging time is about 86%, in which surface roughening contributes more than nanoenhancement in increasing the charging time of the heat sink, which is evident from the individual comparisons made.

Analysis during cooling of the heat sink

This study considers the cooling cycle of the heat sink as a discharging cycle. Discharging time is required by the heat sink to cool down from 70 °C to room temperature. From fig. 8, it can be seen that the discharging time decreases with the addition of nanoparticles. This is due to the high thermal conductivity of the PCM, which aids in faster discharging of internal thermal energy to the surroundings. From the application point of view, it is desirable to have a heat sink with faster discharging. From the results, it was seen that paraffin wax is the best-performing PCM in terms of discharging, too. Grit-blasted heat sinks take the most time

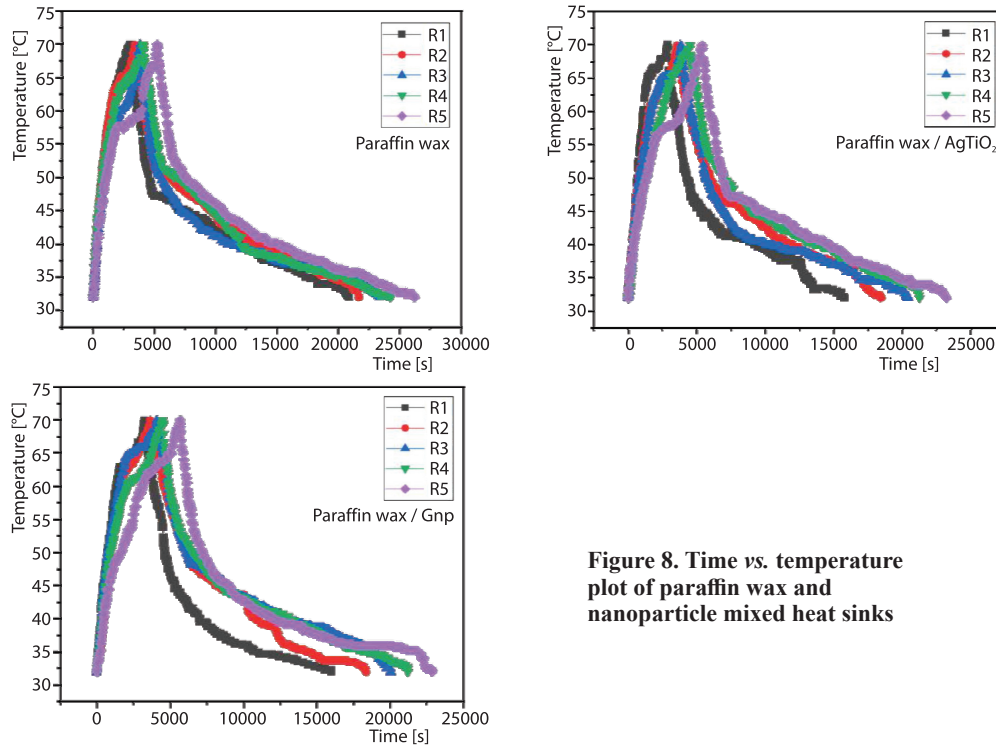


Figure 8. Time vs. temperature plot of paraffin wax and nanoparticle mixed heat sinks

to discharge, followed by base-engraved heat sinks. This is because interior surface roughened heat sinks store more thermal energy because of a higher heat transfer rate to the PCM attained while charging. With increasing R_a values, an increase in discharging time is observed. Hence, it is better to use non-roughened heat sinks than internal surface roughened heat sinks for faster discharging.

Adding graphene nanoparticles to the PCM decreases the discharging time by about 29%. When used with paraffin wax, the base engraved heatsinks and grit-blasted heat sinks have increased the discharging time by 10% and 18%, respectively. When graphene-added PCM is used in base engraved and grit-blasted heat sinks, the discharging time decreases by 10% and 4%, respectively.

Performance analysis of the heat sink

From the heating and cooling cycle of the five heat sinks, it is evident that adding nanoparticles to the PCM improves the performance of the heat sink. Internal surface roughening of the heat sinks is beneficial in charging, but it hinders the effectiveness of the discharging. Defining a mathematically measurable parameter to quantify the heat sink's thermal performance is essential. The charging and discharging time of all fifteen heat sink configurations is represented in matrix form in fig. 9.

The PCM-filled heat sinks suit only pulsed operation electronic devices. The maximum temperature and duty cycle are the significant parameters for measuring the pulsed operation device heat sink performance. Since the maximum temperature is kept fixed, the duty cycle is the only comparable parameter. After knowing the charging and discharging time of all fifteen configurations of the heat sinks, the duty cycle can be calculated from eq. (9). It

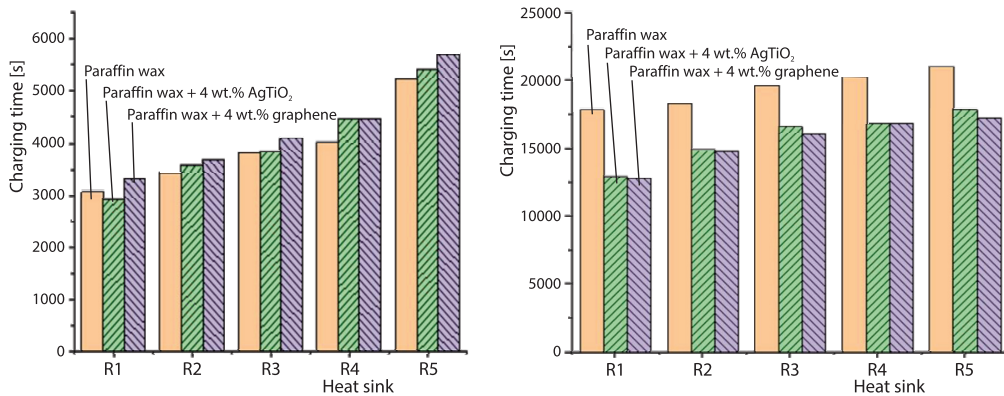


Figure 9. Charging and discharging time of different heat sinks

is represented in fig. 10. The trend observed in this graph is similar to that observed in the case of heat sinks that are charged and discharged. Adding graphene nanoparticles to the PCM increases the duty cycle by about 40%. When used with paraffin wax, base engraved heat-sinks and grit-blasted heat sinks have increased the duty cycle by 11% and 36%, respectively. When graphene-added PCM has used in base impressed and grit-blasted heat sinks, the duty cycle increases by 40% and 71%, respectively. Now, we can conclude that the contribution of grit blasting to the performance of the heat sink is equal to the gift of graphene addition the PCM. Also, increasing the R_a value of the internal surface of the heat sink increases the performance of the heat sink. Overall, graphene-added PCM is better than AgTiO₂-added PCM, and grit blasting is a better technique than base engraving to roughen the internal surfaces of the heat sink. The surface roughness for the heat sink subjected to R5 condition was 15.2 μm . The reasonably large roughness value acted as micro fins. These minuscule fins facilitated the required surface to boost the heat transfer between.

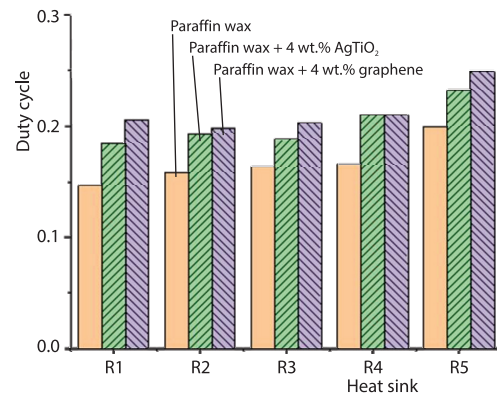


Figure 10. The duty cycle of different heat sinks

Conclusion

From the experiments conducted, it was found that the duty cycle improved from 15-25% by using a hybrid combination of internal grit blasting and thermal conductivity enhancement of paraffin wax and graphene nanoparticles. It was also observed that the performance index increases with an increase in R_a value for any method of roughening and any PCM used. Among the techniques used for roughening, grit blasting has an upper edge over engraving. This is because of the cost-effectiveness and better contribution the performance enhancement of the heat sink. Also, it was seen that graphene-mixed paraffin wax performed better than AgTiO₂-mixed paraffin wax and plain paraffin wax. The improvement in thermal performance occurred because of the higher thermal conductivity of graphene. Hence, the critical inference of all the experiments conducted is that increasing the thermal conductivity of the PCM used in PCM-filled heat sinks and increasing the roughness of the internal surfaces of the heat sink

enhances the heat transfer from the heat sink to the PCM, which ultimately results in improved performance of the heat sink. This heat sink can be used to cool portable electronic components like mobile phones, laptops, monitors, toys and equipment like desktop computers.

References

- [1] Reuben Raj, Cyril, et al. Thermal Performance of NanoEnriched Form-Stable PCM Implanted in a Pin Finned Wall-Less Heat Sink for Thermal Management Application, *Energy Conversion and Management*, 226 (2020), 113466
- [2] Palappan, R., et al., Heating and Cooling Capacity of Phase Change Material Coupled with Screen Mesh Wick Heat Pipe for Thermal Energy Storage Applications, *Thermal Science*, 24 (2020), 2A, pp. 723-734
- [3] Madhaiyan, R., et al. Experimental Study on Heat Transfer Performance of Variable Area Straight Fin Heat Sinks with PCM, *Thermal Science*, 26 (2022), 2A, pp. 983-989
- [4] Lakshmanan, P., et al., Experimental Analysis of Effect of Base with Different Inner Geometries Filled NanoPCM for the Thermal Performance of the Plate Fin Heat Sink, *Thermal Science*, 26 (2022), 2A, pp. 963-968
- [5] Sivapragasam, A., et al., Experimental Investigation on Thermal Performance of Plate Fin Heat Sinks with NanoPCM, *Thermal Science*, 24 (2020), 1B, pp. 437-446
- [6] Lakshmanan, P., et al., Experimental Analysis of Effect of Base with Different Inner Geometries Filled NanoPCM for the Thermal Performance of the Plate Fin Heat Sink, *Thermal Science*, 26 (2022), 2A, pp. 963-968
- [7] Rajesh, B., Balaji, C., Thermal Performance of a PCM Heat Sink under Different Heat Loads: An Experimental Study, *International Journal of Thermal Sciences*, 79 (2024), May, pp. 240-249
- [8] Pal, D., Yogendra, K. J., Melting in a Side Heated Tall Enclosure by a Uniformly Dissipating Heat Source, *International Journal of Heat and Mass Transfer*, 44 (2001), 2, pp. 375-387
- [9] Kandasamy, R., et al., Transient Cooling of Electronics Using Phase Change Material (PCM)-Based Heat Sinks, *Applied Thermal Engineering*, 28 (2008), 8-9, pp. 1047-1057
- [10] Fok, S. C., et al., Cooling of Portable Hand-Held Electronic Devices Using Phase Change Materials in Finned Heat Sinks, *International Journal of Thermal Sciences*, 49 (2010), 1, pp. 109-117
- [11] Yang, Y.-T., Wang, Y. H., Numerical Simulation of 3-D Transient Cooling Application on a Portable Electronic Device Using Phase Change Material, *International Journal of Thermal Sciences*, 51 (2012), Jan., pp. 155-162
- [12] Arulprakasajothi, M., et al., Experimental Investigation of Salinity Gradient Solar Pond with NanoBased Phase Change Materials, *Energy Sources – Part A: Recovery, Utilization, and Environmental Effects*, 45 (2023), 2, pp. 5465-580
- [13] Muthu, G., et al., Performance of Solar Parabolic Dish Thermoelectric Generator with PCM, *Materials Today: Proceedings*, 37 (2021), Part 2, pp. 929-933
- [14] Balakrishnan, R., et al., *Analysis of the Thermal Management of Electronic Equipment by Employing Silicon Carbide NanoPCM-Based Heat Sink*, Environmental Science and Pollution Research, Springer, New York, USA, 2023
- [15] Choi, Da H., et al., Thermal Conductivity and Heat Transfer Performance Enhancement of Phase Change Materials (PCM) Containing Carbon Additives for Heat Storage Application, *International Journal of Refrigeration*, 42 (2014), June, pp. 112-120
- [16] Bahiraei, F., et al., Experimental and Numerical Investigation on the Performance of Carbon-Based Nanoenhanced Phase Change Materials for Thermal Management Applications, *Energy Conversion and Management*, 153 (2017), Dec., pp. 115-128
- [17] Zou, D., et al. Thermal Performance Enhancement of Composite Phase Change Materials (PCM) Using Graphene and Carbon Nanotubes as Additives for the Potential Application in Lithium-Ion Power Battery, *International Journal of Heat and Mass Transfer*, 120 (2018), May, pp. 33-41
- [18] Pahamli, Y., et al., Effect of Nanoparticle Dispersion and Inclination Angle on Melting of PCM in a Shell and Tube Heat Exchanger, *Journal of the Taiwan Institute of Chemical Engineers*, 81 (2017), Dec., pp. 316-334
- [19] Praveen, B., Suresh, S., Experimental Study on Heat Transfer Performance of Neopentyl Glycol/CuO Composite Solid-Solid PCM in TES-Based Heat Sink. Engineering Science and Technology, *International Journal*, 21 (2018), 5, pp. 1086-1094

- [20] Sharma, R. K., *et al.* Thermal Properties and Heat Storage Analysis of Palmitic Acid-TiO₂ Composite as NanoEnhanced Organic Phase Change Material (NEOPCM), *Applied Thermal Engineering*, 99 (2016), Apr., pp. 1254-1262
- [21] Putra, N., *et al.*, Preparation of Beeswax/Multi-Walled Carbon Nanotubes as Novel Shape-Stable Nanocomposite Phase-Change Material for Thermal Energy Storage, *Journal of Energy Storage*, 21 (2019), Feb., pp. 32-39
- [22] He, M., *et al.*, Preparation, Thermal Characterization and Examination of Phase Change Materials (PCM) Enhanced by Carbon-Based Nanoparticles for Solar Thermal Energy Storage, *Journal of Energy Storage*, 25 (2019), 100874
- [23] Zhang, X., *et al.*, Preparation and Thermal Properties of N-Eicosane/NanoSiO₂/Expanded Graphite Composite Phase-Change Material for Thermal Energy Storage, *Materials Chemistry and Physics*, 240 (2020), 122178
- [24] Lawag, R. A., *et al.*, Investigation of PT 58 and PEG-6000-Based Finned Heat Sinks for Thermal Management of Electronics, *Journal of Cleaner Production*, 390 (2023), 136101
- [25] Babar, H., *et al.*, Hydrothermal Performance of Inline and Staggered Arrangements of Airfoil Shaped Pin-Fin Heat Sinks: A Comparative Study, *Thermal Science and Engineering Progress*, 37 (2022), 2023
- [26] Fayyaz, H., *et al.*, Experimental Analysis of NanoEnhanced Phase-Change Material with Different Configurations of Heat Sinks, *Materials*, 15 (2022), 22, 8244